Published in final edited form as:
Nat Neurosci. 2011 June ; 14(6): 711–717. doi:10.1038/nn.2803.

Position-dependent patterning of spontaneous action potentials in immature cochlear inner hair cells

Stuart L. Johnson[1], **Tobias Eckrich**[1], **Stephanie Kuhn**[1], **Valeria Zampini**[1,2], **Christoph Franz**[3], **Kishani M. Ranatunga**[4], **Terri P. Roberts**[4], **Sergio Masetto**[2], **Marlies Knipper**[3], **Corné J. Kros**[4,*], and **Walter Marcotti**[1,*]

[1]Department of Biomedical Science, University of Sheffield, Sheffield, S10 2TN, UK

[2]Department of Physiology, University of Pavia, Pavia, 27100, Italy

[3]Department of Otolaryngology, Tübingen Hearing Research Centre, Laboratory of Molecular Physiology of Hearing, University of Tübingen, D-72076 Tübingen, Germany

[4]School of Life Sciences, University of Sussex, Falmer, Brighton BN1 9QG, UK

Abstract

Spontaneous action potential activity is crucial for mammalian sensory system development. In the auditory system, patterned firing activity has been observed in immature spiral ganglion cells and brain-stem neurons and is likely to depend on cochlear inner hair cell (IHC) action potentials. It remains uncertain whether spiking activity is intrinsic to developing IHCs and whether it shows patterning. We found that action potentials are intrinsically generated by immature IHCs of altricial rodents and that apical IHCs exhibit bursting activity as opposed to more sustained firing in basal cells. We show that the efferent neurotransmitter ACh, by fine-tuning the IHC's resting membrane potential (V_m), is crucial for the bursting pattern in apical cells. Endogenous extracellular ATP also contributes to the V_m of apical and basal IHCs by activating SK2 channels. We hypothesize that the difference in firing pattern along the cochlea instructs the tonotopic differentiation of IHCs and auditory pathway.

The origin and development of neural circuits, including those of sensory systems such as the cochlea and the retina, depend on intrinsic genetic programmes that are coordinated by specific microRNAs[1-2]. While the initial wiring of the sensory circuits involves axon guidance molecules[3,4], their refinement towards mature functional characteristics is hypothesized to be driven by intrinsically-generated (i.e. experience-independent) electrical activity, which occurs during a critical period of development in immature sensory organs[5-7]. Early spontaneous action potential activity has been shown to regulate a variety of cellular responses[8] including the remodelling of synaptic connections [7,9] and ion-channel expression[10]. As well as promoting the survival of immature sensory cells and newly formed connections within the organ, spontaneous action potential activity is believed to serve a more instructive role in sensory refinement[9]. Differences in pattern, which depend on the cell's position within the immature organ, might help establish ordered neural maps of the sensory environment before the onset of experience-driven activity.

[*]To whom correspondence and proofs should be addressed: Dr. Walter Marcotti: Department of Biomedical Science, University of Sheffield, Sheffield, S10 2TN, UK. Tel: +44-114-222-1098, w.marcotti@sheffield.ac.uk or C.J.K (c.j.kros@sussex.ac.uk). .
Author contribution: S.L.J. and W.M. performed most of the experimental work. All authors helped with the collection and analysis of the data. C.F. and M.K. collected immunolabelling data. C.J.K. had the initial idea of using cell-attached recording of IHC APs. W.M., S.L.J and C.J.K. designed the experiments and wrote the paper. All authors discussed the results and commented on the manuscript.
Author Information: The authors declare that they have no competing financial interest.

Europe PMC Funders Author Manuscripts

In the mammalian cochlea, the primary sensory receptor inner hair cells (IHCs), fire spontaneous action potentials[11-15] before the onset of hearing, which in various altricial rodents occurs around postnatal day 12 (P12). Any differences in the pattern of action potential activity as a function of position along the immature cochlea might instruct the functional differentiation of the IHCs themselves[16], the biophysical properties of which are known to vary along the cochlea[17-19], as well as the possible refinement of tonotopic maps in the auditory pathway[20]. In this study we compared action potential activity in apical and basal IHCs and found position-dependent differences in its patterning along the cochlea. Moreover, we found that while ATP is involved in maintaining V_m near the potential at which the Ca^{2+} current begins to activate, the efferent neurotransmitter ACh is likely to be responsible for the burst-like action potential pattern observed specifically in apical IHCs.

Results

In the mammalian cochlea spontaneous spiking activity in immature IHCs has been observed during the first postnatal week[12-14]. Although action potentials (APs) are mainly due to the interplay between a Ca^{2+} and a delayed rectifier K^+ current[14,21], their frequency has been shown to be modulated by other currents that are transiently expressed in immature IHCs: the Na^+ current[14] and a small conductance Ca^{2+} activated K^+ current SK2 (I_{SK2})[16,22]. Action potential activity is also regulated by the efferent neurotransmitter acetylcholine (ACh)[23]. Recently, it has been suggested that early postnatal IHCs have a significantly more hyperpolarized V_m[24,25] than previously reported using whole-cell[12-14] or perforated-patch[16] recordings. As a consequence, it was proposed that IHCs are not intrinsically spontaneously active but that instead APs are only triggered by waves of ATP released from supporting cells in Kölliker's organ[24,25]. These waves were shown to lead to ATP-dependent activation of purinergic receptors in IHCs resulting in a depolarizing inward cation current.

Action potentials occur spontaneously in immature cells

We have investigated the origin of action potential activity in IHCs during the first postnatal week in mice, rats and gerbils at 35-37°C and in perilymph-like extracellular solution (1.3 mM Ca^{2+} and 5.8 mM K^+) using whole-cell current clamp (Fig. 1a) or cell-attached voltage clamp (Fig. 1b). The cell-attached recording technique has the advantage that it preserves the intracellular milieu, including endogenous Ca^{2+} buffers. Therefore, IHC V_m and the frequency and pattern of spontaneous APs should, as closely as possible, represent that *in vivo*. During cell-attached recording, APs manifest as biphasic capacitative currents (Fig. 1b) and could be recorded in nearly all IHCs tested within the first postnatal week. Cell-attached spikes resulted from Ca^{2+}-dependent APs since they were abolished by the application of a Ca^{2+}-free solution (Fig. 1c). Furthermore, the frequency of spikes increased when IHCs were depolarized by extracellular application of a high-K^+ solution (Fig. 1d). Under all conditions tested, the patterns of cell-attached and whole-cell spikes appeared qualitatively the same (Fig. 1). The cell-attached mode allowed spontaneous action potential activity to be recorded for much longer durations (our longest recording was one hour) than whole-cell recording (less than twenty minutes, probably due to Ca^{2+} current rundown), allowing for a more comprehensive analysis. These recordings also represent the first demonstration of long-lasting action potential activity in IHCs, indicative of well-preserved cells with a stable V_m. The action potential activity occurred at the cell's V_m and was not accompanied by any obvious waves of depolarization (Fig. 1, Supplementary Fig. 1) that could be linked to ATP release from Kölliker's organ[24,25]. This confirms our previous studies using both whole-cell[14,21] and perforated patch recordings[16]. Similar responses were observed whether the patch pipette was advanced from the modiolar or strial side of the cochlea, the latter ensuring Kölliker's organ remained entirely intact[24]. However, we noticed that the action potential width in our recordings (half width 3.8 ms in both perforated patch

and whole-cell recordings: Fig. 2a, b) was about 3-9 times shorter than that recently reported[25], suggesting differences in the currents underlying APs between the studies.

To establish the basis for the above mentioned differences, we compared recordings made at room temperature with an intracellular solution containing 10 mM EGTA (as recently used to measure IHC voltage responses[24-26]), to those with our standard conditions of body temperature and 1 mM EGTA. Under the room temperature and 10 mM EGTA condition, we found that I_{SK2} was absent or significantly reduced compared to that measured in 1 mM EGTA (Fig. 2c, d: one-way ANOVA, Tukey test: $P < 0.001$) or using perforated patch (Fig. 2d: $P < 0.01$, overall significance $P < 0.0001$). This indicates that 10 mM EGTA buffers most of the Ca^{2+} entering the IHC before it reaches the SK2 channels. The total outward K^+ current from IHCs recorded with 10 mM EGTA was similar to that obtained in SK2 knockout mice (perforated patch) and when I_{SK2} was abolished using a Ca^{2+}-free extracellular solution[22] (whole-cell) (Fig. 2d). In the absence of I_{SK2} the action potential width was significantly increased compared to that measured in perforated patch recordings or using 1 mM intracellular EGTA (Fig. 2b: one-way ANOVA: $P < 0.0001$). Since I_{SK2} is essential for robust action potential repolarization, its absence affects the ability of an IHC to sustain spiking activity[16,22]. At room temperature and with 10 mM EGTA we also found that the V_m of apical-coil IHCs was significantly more hyperpolarized (−70.4 ± 1.5 mV, n = 11, P3-P4) than that of similar cells recorded at body temperature and using 1 mM EGTA (−58.5 ± 0.4 mV, n = 44, P2-P5, $P < 0.0001$), preventing them from firing spontaneous APs. Moreover, we observed discrete bursts of action potential activity associated with brief periods of cell depolarization (9.4 ± 2.1 mV from five P3 IHCs: Fig. 2e), which were similar to those recently reported under analogous conditions[24-26]. Therefore, to avoid adversely affecting the nature and kinetics of the currents underlying spontaneous action potential activity, we performed all our whole-cell recordings as previously described[14,16,21] (35-37°C; 1 mM intracellular EGTA; in perilymph-like extracellular solution[27]: 1.3 mM Ca^{2+} and 5.8 mM K^+).

The pattern of spontaneous APs varies along the cochlea

To assess possible position-dependent differences in spontaneous action potential activity, we performed cell-attached recordings from IHCs in the apical and basal regions of the immature rat cochlea (Fig. 3a). The firing pattern of apical IHCs appeared organized in bursts (rat: Fig. 3a, b; gerbil: Supplementary Fig. 2a-c) that were less evident in recordings from basal IHCs (rat: Fig. 3a, c). A consequence of the more burst-like pattern in apical rat IHCs was that the mean but not the median spike frequency (mean 0.60 ± 0.09 Hz, median 2.00 ± 0.14 Hz, n = 17) was significantly lower than in basal cells (mean 1.23 ± 0.13 Hz, median 1.80 ± 0.13 Hz, n = 15, $P < 0.001$). In the interspike interval (ISI) histograms (Fig. 3d), the relatively quiet intervals in between the bursts are responsible for the pronounced 'tail' at large ISIs for apical IHCs. We used the coefficient of variation as a quantitative measure of regularity in spontaneous spike firing. The coefficient of variation for a random Poisson process is 1; values <1 indicate more regular activity whereas bursting leads to values >1[28,29]. The coefficient of variation in apical IHCs (2.70 ± 0.24, P2-P5, n = 17) was significantly larger ($P < 0.0001$) than in basal cells (1.16 ± 0.08, P2-P5, n = 15) (Fig. 3e). We have also observed similar apical-to-basal differences in the frequency and pattern of action potential activity in mouse IHCs (Supplementary Fig. 1), suggesting that they are a robust and general feature of mammalian cochlear development. During the first postnatal week, the coefficient of variation remained relatively constant in apical and basal rat IHCs (Fig. 3f) and apical gerbil IHCs (Supplementary Fig. 2), indicating that the difference in spike pattern is not due to the development of basal cells being about one-to-two days ahead of apical cells[30]. Gerbils have an extended low-frequency hearing range in the adult (down to ~200 Hz), compared to both mice and rats (~2-3 kHz). The nevertheless similar

coefficient of variation and frequency in apical IHCs of all three rodent species indicate that the spike pattern relates to the cell's position along the length of the cochlea, rather than to the characteristic frequency of sound to which adult IHCs respond best.

The V_m of mouse apical IHCs (−58.5 ± 0.4 mV, $n = 44$, P2-P5) was found to be significantly more hyperpolarized than that of basal cells (−55.5 ± 0.5 mV, $n = 23$, P3-P5, $P < 0.0001$: see also Fig. 7c:"Ctrl"). When small current injections (14 ± 2 pA, $n = 4$) were applied to apical-coil IHCs, causing them to depolarize by about 3 mV and thus mimicking the V_m of basal cells, their firing activity became more regular (Supplementary Fig. 3). This indicates that the mechanisms underlying the different V_m in apical and basal IHCs are crucial determinants of their different firing patterns.

Concentration-dependent roles for ATP in spiking activity

During the first (but not the second) postnatal week the V_m of immature IHCs (Fig. 4a) is positive to the potential at which the Ca^{2+} current becomes activated (−65 mV[14,31]), so at this stage there is no requirement for ATP-induced depolarization to reach the action potential threshold. Because we did not observe any slow waves of depolarization of V_m associated with spontaneous APs, we sought to distinguish whether endogenous ATP was simply not present or whether the IHCs did not depolarize in response to ATP. When superfused with 100 μM ATP mouse IHCs depolarized (Fig. 4b) to a significantly larger extent in basal than in apical IHCs ($P < 0.0005$: Fig. 4c). ATP reversibly increased the frequency and reduced the height of APs (apical IHCs) or even abolished them (basal IHCs). In the presence of ATP the cell-attached spike amplitude of apical IHCs (7.8 ± 0.3 pA, $n = 6$, Fig. 4d) was reduced by 35 ± 14% ($P < 0.001$) when compared to that of control spikes (12.2 ± 0.8 pA, $n = 6$), presumably as a consequence of IHC depolarization. The spike amplitude histogram shows a clear segregation between spikes recorded before and during the application of ATP (Fig. 4e: obtained from the recording in Fig. 4d). Spikes recorded without extracellularly applied ATP had stable amplitudes (Fig. 4f). This shows that action potential bursts are unlikely to result from waves of ATP-induced IHC depolarization.

Having established that IHCs respond to externally applied ATP under our conditions, we sought to investigate the presence of endogenous ATP by applying TNP-ATP, a specific antagonist for purinergic P2X receptors[32]. The expectation was that IHCs would hyperpolarize if endogenous ATP was present due to the block of inward cation current flowing through P2X receptors. Surprisingly, we found that 10 μM TNP-ATP caused apical (Fig. 5a) and basal (Fig. 5b) IHCs to depolarize instead, reversibly increasing the action potential frequency. Basal IHCs were depolarized more ($P < 0.0005$) than apical cells (Fig. 5c). A qualitatively similar effect was observed when TNP-ATP was used at lower concentrations (1 nM - 1 μM: Supplementary Fig. 4). The depolarizing action of TNP-ATP was confirmed by the increased frequency and reduced height of spikes in cell-attached recordings (Fig. 5d). Apical-coil IHCs were also similarly depolarized (7.8 ± 4.1 mV, $n = 3$) when superfused with the more general purinergic receptor blocker PPADS (50 μM). When recordings were performed using SK2-knockout mice or experimental conditions that prevented the activation of the SK2 current, 10 μM TNP-ATP had no or very little effect on V_m (Fig. 5e, f). This indicates that Ca^{2+} influx into IHCs induced by endogenous ATP is able to activate nearby SK2 channels located at or near the synaptic region (Fig. 5g), thus sustaining a repolarizing outward K^+ current. P2X receptors and SK2 channels showed very close co-localization of about 13 nm (apical IHCs: Fig. 5e) to 18 nm (basal IHCs: Fig. 5f), as calculated from the BAPTA concentrations of 10 mM and 5 mM, respectively, required to uncouple them[22,33]. When experiments were performed at room temperature and using 10 mM EGTA in the intracellular solution (Fig. 5e), TNP-ATP induced IHC depolarization was reduced or absent, indicating that under these conditions the SK2 channels are no longer

coupled to the P2X receptors. It is worth noting that in the presence of 1 mM EGTA the size of the SK2 current, when elicited by depolarization (Fig. 2c), was not affected by the extracellular application of either TNP-ATP ($n = 5$) or PPADS ($n = 3$) (data not shown).

To explain the depolarizing effect of TNP-ATP (Fig. 5) we hypothesized that endogenous ATP (i.e. ATP at very low concentrations) should hyperpolarize IHCs. When P4 apical IHCs were superfused with micromolar concentrations of ATP (3 μM - 100 μM) all 9 mouse IHCs tested were depolarized (Fig. 6a, e). ATP in the 30 nM - 300 nM range caused a small hyperpolarization averaging −2.1 mV (Fig. 6b, e) in 6 out of 22 IHCs. In the remaining 16 IHCs, ATP caused a small depolarization ($n = 9$, Fig. 6c, e) or had no effect ($n = 7$). Superfusion of 3 nM - 10 nM ATP (Fig. 6d, e) had a hyperpolarizing effect (−4.1 ± 0.7 mV, range −0.7 mV to −7 mV) in 9 out of 11 IHCs investigated, with two cells showing no response. This hyperpolarization was prevented when TNP-ATP (10 μM) was superfused together with a low concentration of ATP (3 nM) in six P4 apical IHCs (data not shown). The variable responses at intermediate ATP concentrations are likely to be due to differences in the levels of endogenous ATP in the nanomolar range already present around the IHCs. These findings confirm our observations that endogenous ATP modulates the action potential activity intrinsic to IHCs by activating P2X receptors coupled to SK2 channels located at the synaptic region. These receptors are likely to be different to those responding to high concentrations of ATP (Fig. 4) since in the presence of both TNP-ATP and apamin (to block the P2X receptors and SK2 channels responsible for IHC hyperpolarization) the depolarization induced by 100 μM ATP in apical IHCs (data not shown) remained similar to that recorded when ATP was superfused alone (Fig. 4c).

Role of α9α10 nicotinic ACh receptors in spiking activity

ACh is the main efferent neurotransmitter in the mammalian cochlea that exerts an inhibitory effect on IHC responses before hearing onset[23]. Efferent fibres synapse directly with IHCs mainly during pre-hearing stages of development[34]. Efferent inhibition of IHCs is achieved by Ca^{2+} influx through heteromeric α9α10 nAChRs[35],[36] activating the hyperpolarizing SK2 current[22],[23],[37].

We investigated whether endogenously released ACh had a direct role in modulating intrinsic action potential activity by superfusing spontaneously spiking IHCs with the specific α9α10 nAChR blocker strychnine[38]. Strychnine (10 μM) caused a small IHC depolarization, sufficient to change the bursting firing pattern characteristic of apical cells into a more sustained activity (Fig. 7a, b). In the presence of strychnine (1 μM - 10 μM), the V_m of apical IHCs (control −58.5 ± 0.4 mV, $n = 44$; strychnine: −54.8 ± 0.7 mV, $n = 6$) was more depolarized and similar to that of basal cells (control: −55.5 ± 0.5 mV, $n = 23$; strychnine: −54.1 ± 0.7 mV, $n = 4$, Fig. 7c). During strychnine application the coefficient of variation (Fig. 7d) and mean frequency (Fig. 7e) of action potential activity in apical IHCs were similar to those of basal cells. Moreover, the V_m and action potential properties of apical and basal IHCs in the presence of strychnine did not differ significantly from those of control basal cells (one-way ANOVA, Fig. 7c-e). Cell-attached spike recordings further confirmed that strychnine increased the frequency and decreased the coefficient of variation of action potentials in apical IHCs (Fig. 7f, g) and that the efferent neurotransmitter ACh inhibited IHC firing activity (Fig. 7h).

The more pronounced effect of strychnine on apical-coil IHCs could in principle be due to larger currents induced by ACh or the presence of more endogenously released ACh than in the basal coil. In the presence of 5 mM BAPTA, which uncouples most of the SK2 channels from the ACh receptors[22], the inward current induced by 30 μM ACh measured at −84 mV[39] was similar between apical (−63 ± 7 pA, $n = 5$) and basal (−92 ± 24 pA, $n = 6$) P3

IHCs, suggesting a comparable number of ACh receptors. Moreover, α9α10 nAChRs are likely to be similarly colocalized to SK2 channels in both cochlear regions since 30 μM ACh caused an equivalent degree of hyperpolarization in both apical (14.0 ± 0.1 mV, $n = 3$) and basal (13.0 ± 0.7 mV, $n = 3$) P5 IHCs. The conclusion is that endogenously released ACh is likely to be much more prevalent in the apical coil.

We verified that the effect of strychnine was due to ACh released by the efferent system by attempting to block its release by either preventing action potential activity in the efferent terminals using the Na^+ channel blocker TTX or by indirectly exhausting exocytosis from the efferent terminals by inhibiting endocytosis of ACh-filled vesicles with dynasore[40]. In the continuous presence of TTX or dynasore (Supplementary Fig. 5), 10 μM strychnine had very little or no depolarizing effect on all apical IHCs tested (TTX: 0.3 ± 0.1 mV, $n = 11$, P4; dynasore: 1.1 ± 0.6 mV, $n = 4$, P4), when compared to that obtained in control conditions (Fig. 7c: 3.7 mV). The coefficient of variation and mean frequency of action potential activity in apical IHCs in the presence of TTX or dynasore (coefficient of variation: 0.7 ± 0.1; frequency: 5.0 ± 0.4 Hz, $n = 8$, Supplementary Fig. 5) were similar to those of control basal cells (Fig. 7d, e, respectively). These findings indicate that ACh released from the efferent terminals is essential for setting the bursting firing pattern in apical IHCs by tuning their V_m to a value more hyperpolarized than that of basal cells.

Discussion

We show that the action potential activity during the first postnatal week in immature IHCs of altricial rodents is intrinsically generated by the cells themselves, but modulated in different ways by inhibitory effects due to ACh and ATP released near the IHCs. The frequency and pattern of this spontaneous activity differs between apical and basal regions of the cochlea, with apical IHCs showing a bursting pattern and basal IHCs a more regular pattern with a higher mean frequency. Patterned spontaneous action potentials have been observed before the onset of hearing in mammalian spiral ganglion cells[28],[41] and auditory brain stem neurons in the chick, where position dependence of their frequency was noted[42]. The difference in pattern of spiking activity we have shown along the immature cochlea would be appropriate for guiding tonotopically the functional differentiation of IHCs[17-19], the specific re-organization of synaptic connections[43] and possibly the refinement of sensory maps along the auditory pathway before the onset of experience-driven activity[20],[42].

An important question is: what determines the patterning of IHC action potentials and the differences in pattern, bursting-like versus more sustained firing, along the cochlea? IHC action potential activity is known to be modulated by the inhibitory efferent neurotransmitter ACh[23],[44] and ATP released from supporting cells[24]. Our experiments with the ACh receptor blocker strychnine indicate that spontaneous release of ACh from efferent nerve fibres[23], via the indirect activation of SK2 channels, keeps apical IHCs more hyperpolarized than basal cells. The physiological consequence of this is that, by fine-tuning the V_m of apical IHCs, ACh has a specific role in determining the bursting-like action potential pattern in these cells (Supplementary Fig. 6). Although we have demonstrated that endogenous ACh originates from the efferent fibres, and that this release is more pronounced in the apical coil of the cochlea, it is not known whether ACh is itself released in bursts or how this pathway normally operates in the intact animal. Previous *in vivo* studies suggest that input to IHCs from the cholinergic efferent feedback system could be involved in generating patterned activity in auditory nerve afferents[45],[46].

ATP also affects IHC action potential activity during the first postnatal week, but in a more complex way than previously thought. Higher concentrations of ATP (in the order of μM) depolarize the IHCs as previously described[24], presumably via $P2X_2$ receptors localized at

the cell's cuticular plate[47] (Supplementary Fig. 6). However, we have shown that endogenous ATP around IHCs has, similar to ACh, a hyperpolarizing effect on their V_m by activating IHC P2X receptors that indirectly open co-localized SK2 channels present at or near the cell's presynaptic site (Supplementary Fig. 6). $P2X_7$ and $P2X_3$ are known to be transiently expressed in developing IHCs[47]. The low nanomolar sensitivity of the P2X receptors to TNP-ATP indicates that $P2X_3$ is the most likely candidate to mediate the hyperpolarizing ATP responses in immature cells[32]. $P2X_3$ receptors show an apical to basal expression gradient along the mouse cochlea (low to high)[48]. This could explain the more pronounced effects of ATP in basal IHCs, which have more sustained action potential firing and may thus require additional assistance in robustly repolarizing their membrane potential. Recordings from guinea-pig IHCs show that both hyperpolarizing and depolarizing effects of ATP also occur in the mature cochlea[49], indicative of other, non-developmental, roles.

Tonotopic differences in IHC activity during the first postnatal week could be important for refining the auditory neural circuits in the brainstem, most of which is completed during this time window[20]. From the second postnatal week intrinsic IHC activity disappears due to a progressive hyperpolarization of V_m. At this time, bursts of action potentials elicited by waves of ATP released from supporting cells[24] could be important for coordinating activity in adjacent IHCs. Developmental changes in the mechanisms underlying patterned activity have been found in the retina, spinal cord and hippocampus[7], to which the cochlea can now probably be added. We have shown that there are numerous influences on IHC action potential activity that together exert tight control over the IHCs' intrinsically generated firing pattern as a function of position along the immature cochlea. The need for such elaborate control over the V_m of IHCs points to the crucial importance of their firing activity during cochlear development.

Supplementary Material

Refer to Web version on PubMed Central for supplementary material.

Acknowledgments

This work was supported by project grants from the Wellcome Trust (088719) and RNID (G41) to W.M. and an MRC programme grant to C.J.K. SK2-knockout mice were obtained from J.P. Adelman. W.M. is a Royal Society University Research Fellow.

Appendix

Methods

Electrophysiology

Apical and basal coil inner hair cells (IHCs) from the mouse ($n = 338$), rat ($n = 43$) and gerbil ($n = 27$) were studied in acutely dissected organs of Corti from postnatal day 2 (P2) to P11, where the day of birth is P0. Animals were killed by cervical dislocation in accordance with UK Home Office regulations. Cochleae were dissected as previously described[21] in normal extracellular solution (in mM): 135 NaCl, 5.8 KCl, 1.3 $CaCl_2$, 0.9 $MgCl_2$, 0.7 NaH_2PO_4, 5.6 D-glucose, 10 Hepes-NaOH, 2 sodium pyruvate, amino acids and vitamins (pH 7.5; osmolality ~308 mmol kg^{-1}). Superfusion of IHCs with a Ca^{2+}-free solution, 15 mM K^+, 3 nM-100 μM ATP, 1 nM-10 μM TNP-ATP, 50 μM PPADS, 300 nM TTX (Tocris, UK), 10-100 μM ACh, 1-10 μM strychnine, 100 μM dynasore (Sigma) was performed with a multi-barrelled pipette positioned close to the patched cells. TTX or dynasore were applied for at least 10-20 minutes before using either strychnine or ACh (Supplementary Fig. 5). The spike amplitude was normally distributed in control

experiments and best fitted with a single Gaussian (Fig. 4e, f). In experiments in which ATP was extracellularly applied, the spike amplitude distribution was best fitted with two Gaussian functions.

The pipette solution used for cell-attached recordings contained (in mM): 140 NaCl, 5.8 KCl, 1.3 $CaCl_2$, 0.9 $MgCl_2$, 0.7 NaH_2PO_4, 5.6 D-glucose, 10 Hepes-NaOH (pH 7.5). The whole-cell pipette solution contained (mM): 131 KCl, 3 $MgCl_2$, 1 EGTA-KOH, 5 Na_2ATP, 5 Hepes-KOH, 10 sodium phosphocreatine (pH 7.3). In some cases 1 mM EGTA was replaced by 10 mM EGTA or different BAPTA concentrations (5 mM and 10mM) and KCl was adjusted to keep the osmolality constant. The following KCH_3SO_3-based intracellular solution (in mM: 134 KCH_3SO_3, 1 $MgCl_2$, 10 EGTA-KOH, 2 Na_2ATP, 20 Hepes-KOH, 0.2 Na_2GTP, pH 7.3) was used for recording from apical-coil IHCs in order to test whether the different experimental conditions previously used elsewhere[24-26] to record action potential activity from IHCs (mainly room temperature and 10 mM intracellular EGTA) affected the cells' responses. Data from perforated-patch experiments (Fig. 2) were obtained by analyzing recordings from IHCs previously obtained for Refs [16], [22]. Patch pipettes were made from Soda glass capillaries (Harvard Apparatus Ltd) and coated with surf wax (SexWax, Mr Zoggs) to minimise the fast transient due to the patch pipette capacitance. Unless otherwise stated, experiments were performed close to body temperature (35-37°C) and with 1.3 mM Ca^{2+} and 5.8 mM K^+ in the extracellular solution, similar to those of perilymph[27], to try and approach normal physiological conditions as best as possible.

Electrophysiological recordings were made using Optopatch (Cairn Research Ltd, UK) or Axopatch 200B (Molecular Devices, USA) amplifiers. Data acquisition was controlled by pClamp software using Digidata 1322A or 1440A boards (Molecular Devices, CA, USA). Recordings were low-pass filtered at 2.5 kHz (8-pole Bessel) and sampled at 5 kHz. Cell-attached action potential recordings (seal resistance was 1.80 ± 0.05 GO, $n = 149$) were filtered at 10 kHz and sampled at 20 kHz. Some were in addition low-pass filtered offline at 500 Hz (8-pole Bessel) using Clampfit. Data analysis was performed using Origin software (OriginLab, MA, USA). The Mini Analysis Program (Synaptosoft Inc. NJ, USA) was used to detect biphasic spike events, to calculate their frequency and to analyze interspike intervals (ISI) and amplitudes. The action potential frequency was calculated as the reciprocal of the mean ISI for each cell and an indication of the spread of ISI values about the mean was obtained by calculating the coefficient of variation, equal to the standard deviation divided by the mean. Whole-cell membrane potentials (V) were corrected for the liquid junction potential of −4 mV (KCl-based intracellular) or −10 mV (KCH_3SO_3-based intracellular), measured between electrode and bath solutions.

Statistical analysis

Statistical comparisons of means were made by Student's two-tailed t-test or, for multiple comparisons, one-way ANOVA followed by the Tukey test. Means are quoted ± s.e.m. and $P < 0.05$ was used as the criterion for statistical significance.

Immuno-fluorescence labelling

Cochleae from immature mice were used to prepare cryosections for immuno-fluorescence microscopy and processed as previously described[50]. Briefly, cochleae were dissected and fixed for 2 h with 2% paraformaldehyde (w/v), embedded and cryosectioned at a thickness of 10 μm. Sections were mounted with Vectashield medium with DAPI (Vector Laboratories). Antibodies to SK2 channels (rabbit, Sigma, diluted 1:50) and the IHC marker otoferlin (mouse, Abcam, diluted 1:100) were used. Primary antibodies were detected with Cy3-conjugated (Jackson ImmunoResearch Laboratories) or Alexa Fluor 488–conjugated secondary antibodies (Molecular Probes). Sections were viewed using an Olympus BX61

microscope equipped with motorized z axis and epifluorescence illumination. Images were acquired using a CCD camera and analyzed with cellSense Dimension software (OSIS). To display SK2 channel distribution, cochlea slices were imaged over a distance of several μm to cover the IHC width in an image-stack along the z axis (z stack) followed by three-dimensional deconvolution (cellSense Dimensions, OSIS). Fig. 5g shows composite images, which represent the maximum intensity projection over all layers of the z stack.

References

1. Conte I, Carrella S, Avellino R, Karali M, Marco-Ferreres R, et al. miR-204 is required for lens and retinal development via Meis2 targeting. Proc. Natl. Acad. Sci. USA. 2010; 107:15491–15496. [PubMed: 20713703]
2. Kuhn S, Johnson SL, Furness DN, Chen J, Ingham N, et al. miR-96 regulates the progression of differentiation in mammalian cochlear inner and outer hair cells. Proc. Natl. Acad. Sci. USA. 2011; 108:2355–2360. [PubMed: 21245307]
3. Huberman AD, Feller MB, Chapman B. Mechanisms underlying development of visual maps and receptive fields. Annu. Rev. Neurosci. 2008; 31:479–509. [PubMed: 18558864]
4. Fekete DM, Campero AM. Axon guidance in the inner ear. Int. J. Dev. Biol. 2007; 51:549–56. [PubMed: 17891716]
5. Katz LC, Shatz CJ. Synaptic activity and the construction of cortical circuits. Science. 1996; 274:1133–1138. [PubMed: 8895456]
6. Stellwagen D, Shatz CJ. An instructive role for retinal waves in the development of retinogeniculate connectivity. Neuron. 2002; 33:357–367. [PubMed: 11832224]
7. Blankenship AG, Feller MB. Mechanisms underlying spontaneous patterned activity in developing neural circuits. Nat. Rev. Neurosci. 2010; 11:18–29. [PubMed: 19953103]
8. Berridge MJ, Lipp P, Bootman MD. The versatility and universality of calcium signalling. Nat. Rev. Mol. Cell. Biol. 2000; 1:11–21. [PubMed: 11413485]
9. Zhang LI, Poo M. Electrical activity and development of neural circuits. Nat. Neurosci. 2001; 4:1207–1214. [PubMed: 11687831]
10. Moody WJ, Bosma MM. Ion channel development, spontaneous activity, and activity-dependent development in nerve and muscle cells. Physiol. Rev. 2005; 85:883–941. [PubMed: 15987798]
11. Kros CJ, Ruppersberg JP, Rüsch A. Expression of a potassium current in inner hair cells during development of hearing in mice. Nature. 1998; 394:281–284. [PubMed: 9685158]
12. Beutner D, Moser T. The presynaptic function of mouse cochlear inner hair cells during development of hearing. J. Neurosci. 2001; 21:4593–4599. [PubMed: 11425887]
13. Glowatzki E, Fuchs PA. Transmitter release at the hair cell ribbon synapse. Nat. Neurosci. 2002; 5:147–154. [PubMed: 11802170]
14. Marcotti W, Johnson SL, Rüsch A, Kros CJ. Sodium and calcium currents shape action potentials in immature mouse inner hair cells. J. Physiol. 2003; 552:743–761. [PubMed: 12937295]
15. Brandt N, Kuhn S, Münkner S, Braig C, Winter H, et al. Thyroid hormone deficiency affects postnatal spiking activity and expression of Ca^{2+} and K^{+} channels in rodent inner hair cells. J. Neurosci. 2007; 27:3174–3186. [PubMed: 17376979]
16. Johnson SL, Adelman JP, Marcotti W. Genetic deletion of SK2 channels in mouse inner hair cells prevents the developmental linearization in the Ca^{2+} dependence of exocytosis. J. Physiol. 2007; 583:631–646. [PubMed: 17627990]
17. Johnson SL, Forge A, Knipper M, Münkner S, Marcotti W. Tonotopic variation in the calcium dependence of neurotransmitter release and vesicle pool replenishment at mammalian auditory ribbon synapses. J. Neurosci. 2008; 28:7670–7678. [PubMed: 18650343]
18. Johnson SL, Marcotti W. Biophysical properties of $Ca_V1.3$ calcium channels in gerbil inner hair cells. J. Physiol. 2008; 586:1029–1042. [PubMed: 18174213]
19. Johnson SL, Franz C, Knipper M, Marcotti W. Functional maturation of the exocytotic machinery at gerbil hair cell ribbon synapses. J. Physiol. 2009; 587:1715–1726. [PubMed: 19237422]

20. Kandler K, Clause A, Noh J. Tonotopic reorganization of developing auditory brainstem circuits. Nat. Neurosci. 2009; 12:711–717. [PubMed: 19471270]
21. Marcotti W, Johnson SL, Holley MC, Kros CJ. Developmental changes in the expression of potassium currents of embryonic, neonatal and mature mouse inner hair cells. J. Physiol. 2003; 548:383–400. [PubMed: 12588897]
22. Marcotti W, Johnson SL, Kros CJ. A transiently expressed SK current sustains and modulates action potential activity in immature mouse inner hair cells. J. Physiol. 2004; 560:691–708. [PubMed: 15331671]
23. Glowatzki E, Fuchs PA. Cholinergic synaptic inhibition of inner hair cells in the neonatal mammalian cochlea. Science. 2000; 288:2366–2368. [PubMed: 10875922]
24. Tritsch NX, Yi E, Gale JE, Glowatzki E, Bergles DE. The origin of spontaneous activity in the developing auditory system. Nature. 2007; 450:50–55. [PubMed: 17972875]
25. Tritsch NX, Bergles DE. Developmental regulation of spontaneous activity in the Mammalian cochlea. J. Neurosci. 2010; 30:1539–1550. [PubMed: 20107081]
26. Tritsch NX, Rodríguez-Contreras A, Crins TT, Wang HC, Borst JG, et al. Calcium action potentials in hair cells pattern auditory neuron activity before hearing onset. Nat. Neurosci. 2010; 13:1050–1052. [PubMed: 20676105]
27. Wangemann, P.; Schacht, J. Homeostatic mechanisms in the cochlea. In: Dallos, P.; Popper, A.; Fay, R., editors. The cochlea. Springer; New York: 1996. p. 130-185.
28. Sonntag M, Englitz B, Kopp-Scheinpflug C, Rübsamen R. Early postnatal development of spontaneous and acoustically evoked discharge activity of principal cells of the medial nucleus of the trapezoid body: an in vivo study in mice. J. Neurosci. 2009; 29:9510–9520. [PubMed: 19641114]
29. Jones TA, Jones SM. Spontaneous activity in the statoacoustic ganglion of the chicken embryo. J. Neurophysiol. 2000; 83:1452–1468. [PubMed: 10712472]
30. Kros CJ. How to build an inner hair cell: challenges for regeneration. Hear. Res. 2007; 227:3–10. [PubMed: 17258412]
31. Zampini V, Johnson SL, Franz C, Lawrence ND, Münkner S, et al. Elementary properties of $Ca_V1.3$ Ca^{2+} channels expressed in mouse cochlear inner hair cells. J. Physiol. 2010; 588:187–199. [PubMed: 19917569]
32. North RA, Surprenant A. Pharmacology of cloned P2X receptors. Annu. Rev. Pharmacol. Toxicol. 2000; 40:563–580. [PubMed: 10836147]
33. Neher E. Vesicle pools and Ca^{2+} microdomains: new tools for understanding their roles in neurotransmitter release. Neuron. 1998; 20:389–399. [PubMed: 9539117]
34. Sobkowicz, HM. The development of innervation in the organ of Corti. In: Romand, R., editor. Development of Auditory and Vestibular Systems 2. Elsevier; Amsterdam: 1992. p. 59-100.
35. Elgoyhen AB, Vetter DE, Katz E, Rothlin CV, Heinemann SF, et al. alpha10: a determinant of nicotinic cholinergic receptor function in mammalian vestibular and cochlear mechanosensory hair cells. Proc. Natl. Acad. Sci. USA. 2001; 98:3501–3506. [PubMed: 11248107]
36. Maison SF, Luebke AE, Liberman MC, Zuo J. Efferent protection from acoustic injury is mediated via alpha9 nicotinic acetylcholine receptors on outer hair cells. J. Neurosci. 2002; 22:10838–10846. [PubMed: 12486177]
37. Katz E, Elgoyhen AB, Gomez-Casati ME, Knipper M, Vetter DE, et al. Developmental regulation of nicotinic synapses on cochlear inner hair cells. J. Neurosci. 2004; 24:7814–7820. [PubMed: 15356192]
38. Elgoyhen AB, Johnson DS, Boulter J, Vetter DE, Heinemann S. α9: an acetylcholine receptor with novel pharmacological properties expressed in rat cochlear hair cells. Cell. 1994; 79:705–715. [PubMed: 7954834]
39. Evans MG. Acetylcholine activates two currents in guinea-pig outer hair cells. J. Physiol. 1996; 491:563–578. [PubMed: 8866879]
40. Macia E, Ehrlich M, Massol R, Boucrot E, Brunner C, et al. Dynasore, a cell-permeable inhibitor of dynamin. Dev. Cell. 2006; 10:839–850. [PubMed: 16740485]

41. Jones TA, Leake PA, Snyder RL, Stakhovskaya O, Bonham B. Spontaneous discharge patterns in cochlear spiral ganglion cells before the onset of hearing in cats. J. Neurophysiol. 2007; 98:1898–1908. [PubMed: 17686914]

42. Lippe WR. Relationship between frequency of spontaneous bursting and tonotopic position in the developing avian auditory system. Brain Res. 1995; 703:205–213. [PubMed: 8719634]

43. Pujol, R.; Lavigne-Rebillard, M.; Lenoir, M. Development of the Auditory System. Rubel, EW., et al., editors. Springer; New York: 1998. p. 146-192.

44. Goutman JD, Fuchs PA, Glowatzki E. Facilitating efferent inhibition of inner hair cells in the cochlea of the neonatal rat. J. Physiol. 2005; 566:49–59. [PubMed: 15878942]

45. Walsh, EJ.; Romand, R. Functional development of the cochlea and the cochlear nerve. In: Romand, R., editor. Development of auditory and vestibular systems 2. Elsevier; Amsterdam: 1992. p. 161-210.

46. Köppl C. Spontaneous generation in early sensory development. Focus on “spontaneous discharge patterns in cochlear spiral ganglion cells before the onset of hearing in cats.”. J. Neurophysiol. 2007; 98:1843–1844. [PubMed: 17686910]

47. Housley GD, Marcotti W, Navaratnam D, Yamoah EN. Hair cells - beyond the transducer. J. Membr. Biol. 2006; 209:89–118. [PubMed: 16773496]

48. Huang LC, Ryan AF, Cockayne DA, Housley GD. Developmentally regulated expression of the $P2X_3$ receptor in the mouse cochlea. Histochem. *Cell Biol.*. 2006; 125:681–692. [PubMed: 16341871]

49. Sugasawa M, Erostegui C, Blanchet C, Dulon D. ATP activates non-selective cation channels and calcium release in inner hair cells of the guinea-pig cochlea. J. Physiol. 1996; 491:707–718. [PubMed: 8815205]

50. Heidrych P, Zimmermann U, Kuhn S, Franz C, Engel J, et al. Otoferlin interacts with myosin VI: implications for maintenance of the basolateral synaptic structure of the inner hair cell. Hum. Mol. Genet. 2009; 18:2779–2790. [PubMed: 19417007]

Europe PMC Funders Author Manuscripts

Europe PMC Funders Author Manuscripts

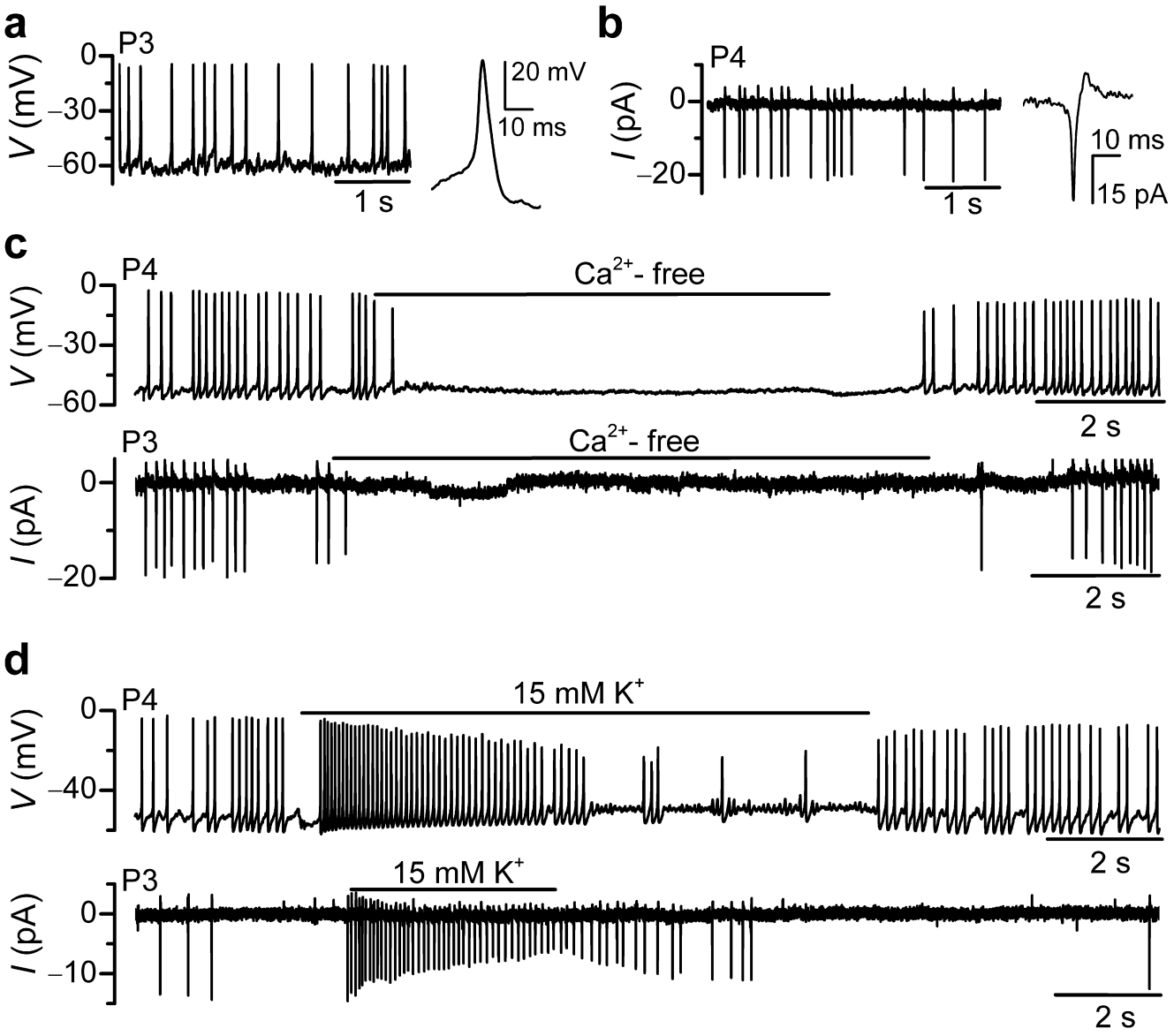

Figure 1. Cell-attached spikes result from spontaneous APs

(**a** and **b**), Spontaneous APs recorded with whole-cell current clamp and cell-attached voltage clamp, respectively. Right panels show an action potential on an expanded time-scale. (**c** and **d**), Whole-cell (top panels) and cell-attached (bottom panels) recordings of spontaneous APs in mouse apical-coil IHCs during the application of a Ca^{2+}-free solution containing 0.5 mM EGTA (**c**), a condition that abolishes this activity[14]. During the perfusion of a solution containing 15 mM K^+ (**d**) IHCs depolarized causing the frequency of spikes to increase while their amplitude declined. In this and the following figures, the duration of substance application is indicated by the horizontal line above the recording.

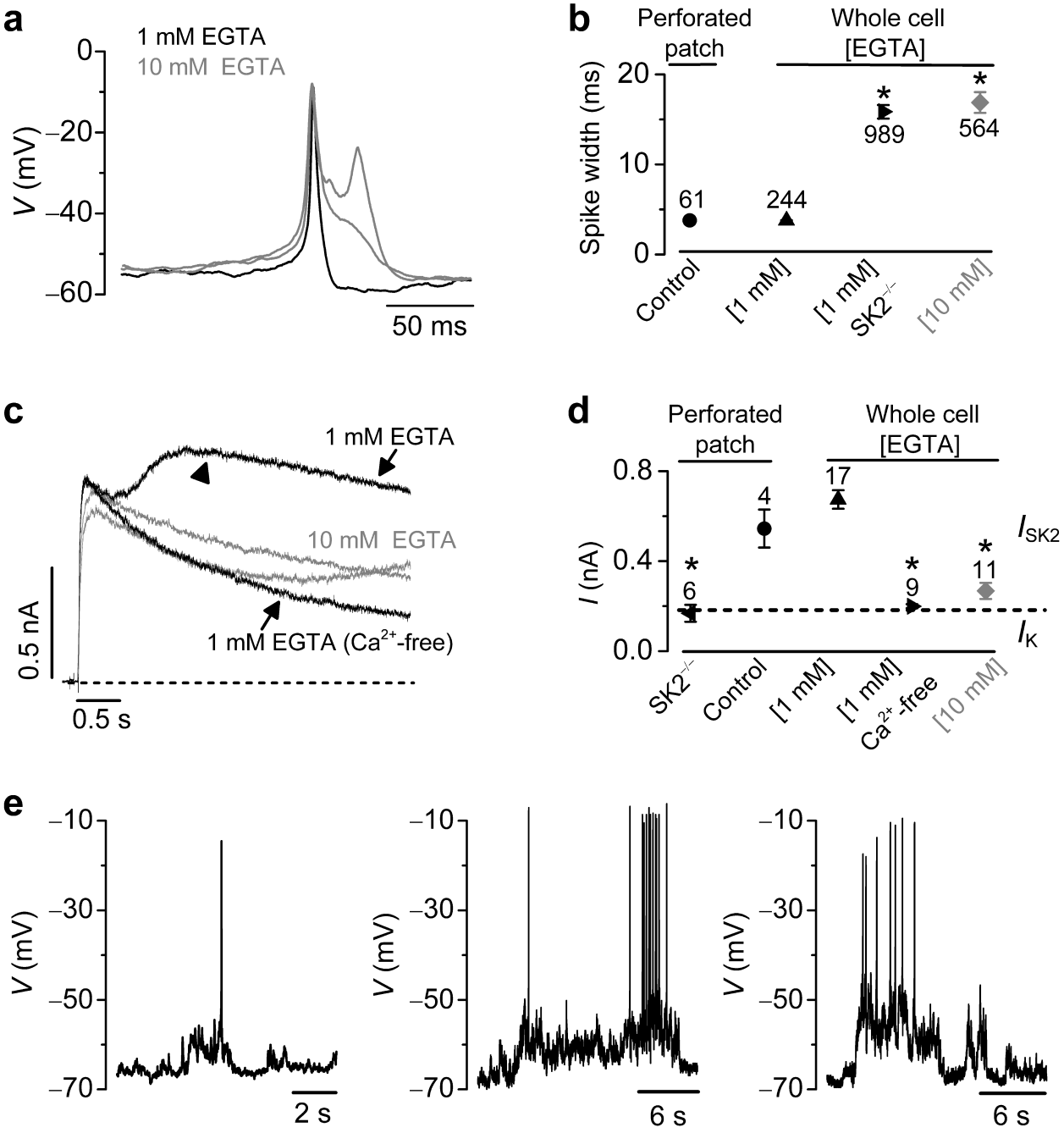

Figure 2. Spontaneous action potentials in IHCs require physiological recording conditions

(**a**), Spontaneous APs recorded from mouse IHCs maintained at 35-37°C and using 1 mM intracellular EGTA[14,16,21] (black traces) or at room temperature using 10 mM EGTA[24-26] (grey). (**b**), Width of the APs measured at 50% between the peak and the after-hyperpolarization. Action potential width in 10 mM EGTA (n = 9, P3-P4) was similar to that measured in IHCs from SK2 knockout mice (SK2$^{-/-}$: n = 9, P4) but larger than that obtained in perforated patch and whole-cell with 1 mM EGTA (n = 5, P3-P7). Number above the symbols indicates the APs analyzed. In this and the following figures, error bars indicates s.e.m. (**c**), Currents in voltage clamp obtained using 1 mM EGTA before and

during the superfusion of a Ca^{2+}-free solution, a condition that abolishes I_{SK2}[16,22] (arrowhead). Recordings were obtained by applying 4 s voltage steps to −10 mV from a holding potential of either −74 mV or −84 mV[22]. In the presence of 10 mM EGTA (Ref: [24-26]), I_{SK2} was absent or largely reduced. (**d**), Size of the total K^+ current (I_K:delayed rectifier and I_{SK2}) from IHCs under different recording conditions. Dashed horizontal line indicates that I_{SK2} is normally superimposed onto I_K. Asterisks indicate significance compared to control. (**e**), At room temperature and using 10 mM EGTA single or bursts of APs were elicited by slow periods of membrane depolarization.

Europe PMC Funders Author Manuscripts

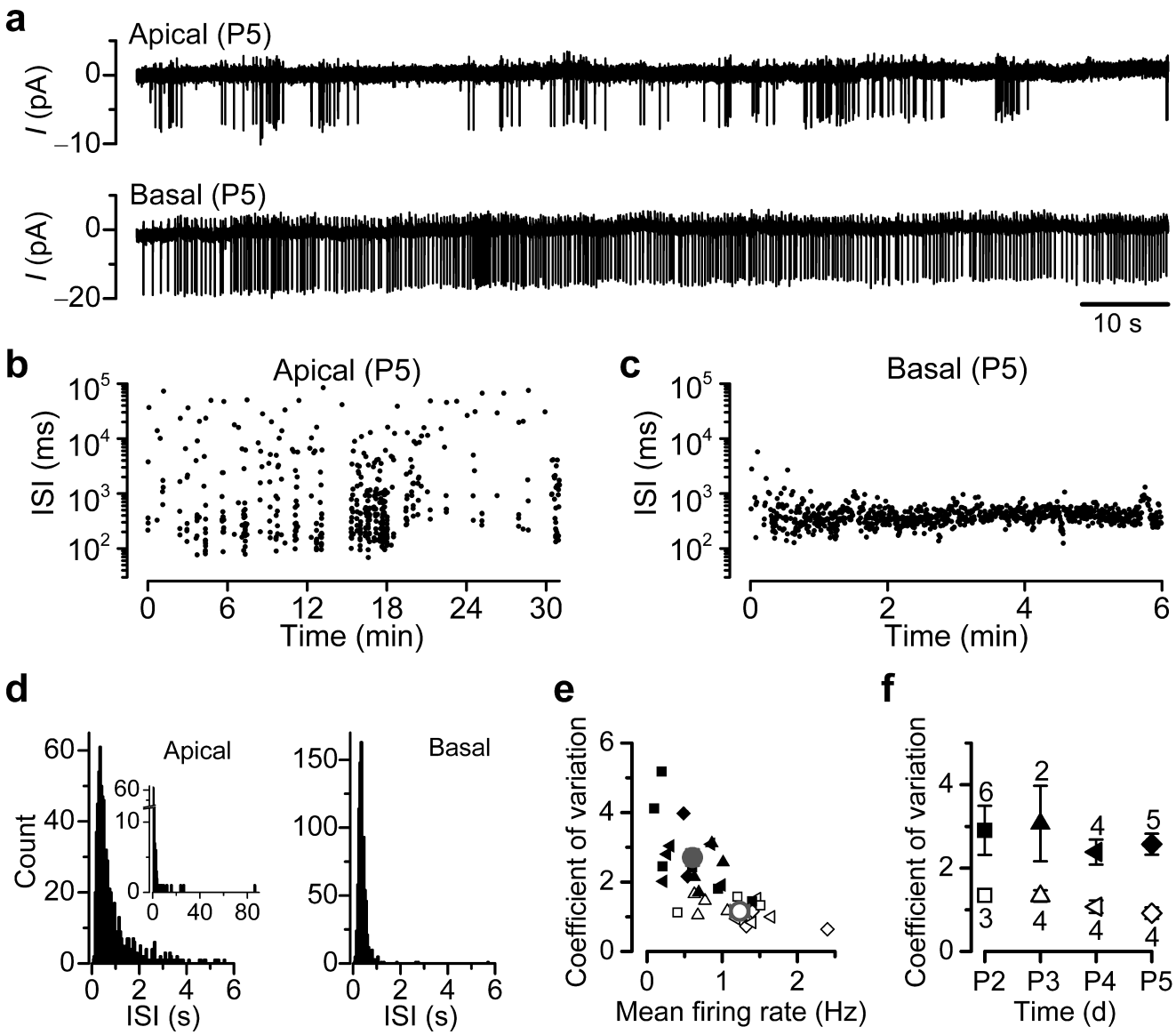

Figure 3. Patterning of spontaneous spiking activity in apical and basal IHCs

(**a**), Cell-attached recordings of spontaneous spikes from an apical and basal rat IHC (120 s out of: apical 31 min; basal 6 min). (**b** and **c**), ISIs as a function of time from the same apical and basal IHCs shown in **a** (mean frequency: apical 0.26 Hz, basal 2.40 Hz; median frequency: 2.32 Hz, 2.68 Hz; coefficient of variation: 2.8, 0.65). The bursting nature of spiking activity in apical IHCs (**b**) is indicated by periodic increases in spiking rate in between silent/reduced activity. In basal IHCs (**c**) spike discharge was more continuous and ISIs were less variable than in apical cells. (**d**), ISI histograms (bin size 50 ms) from the same IHCs shown in **a**. Inset shows the full scale x-axis for the apical IHC. The mode was 0.35 ms for both the apical and basal IHCs. (**e**), Coefficient of variation from each IHC against their firing rate (apical, closed symbols: basal, open symbols; averages in grey). (**f**), Average coefficient of variation as a function of postnatal age. Symbols are as in **e**. IHCs (P2-P5) used for analysis in **e** and **f** were: 17 apical (recording time: 3.6 hrs, 5726 spikes) and 15 basal (1.2 hrs, 5504 spikes).

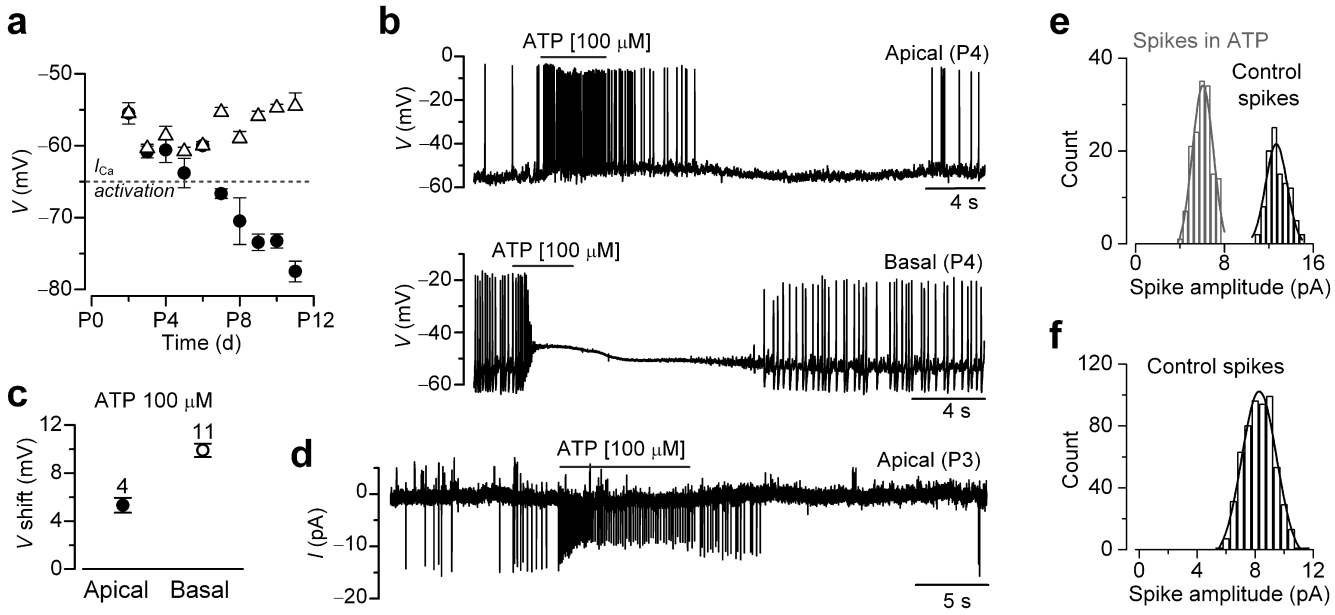

Figure 4. Modulation of action potential activity by superfusing ATP

(**a**), V_m of immature apical IHCs (closed symbols) measured with whole-cell recording. Open triangles indicate the membrane potential threshold required for triggering APs (n = 68, P2-P11). (**b**), ATP increased the action potential frequency in early postnatal apical (upper panel) and basal (lower panel) IHCs, using whole-cell recordings. (**c**), Shift in V_m when apical and basal IHCs were superfused with 100 μM ATP. (**d**), ATP increased spike frequency and decreased their height in apical IHCs using cell-attached recordings. (**e**), Histograms (bin size 0.5 pA) showing the spike amplitude before and during the superfusion of ATP from the same IHC shown in **d** (recording time: 514 s, 377 spikes). (**f**), Spike amplitude histogram from an apical IHC in the absence of exogenous ATP (recording time: 869 s, 748 spikes).

Europe PMC Funders Author Manuscripts

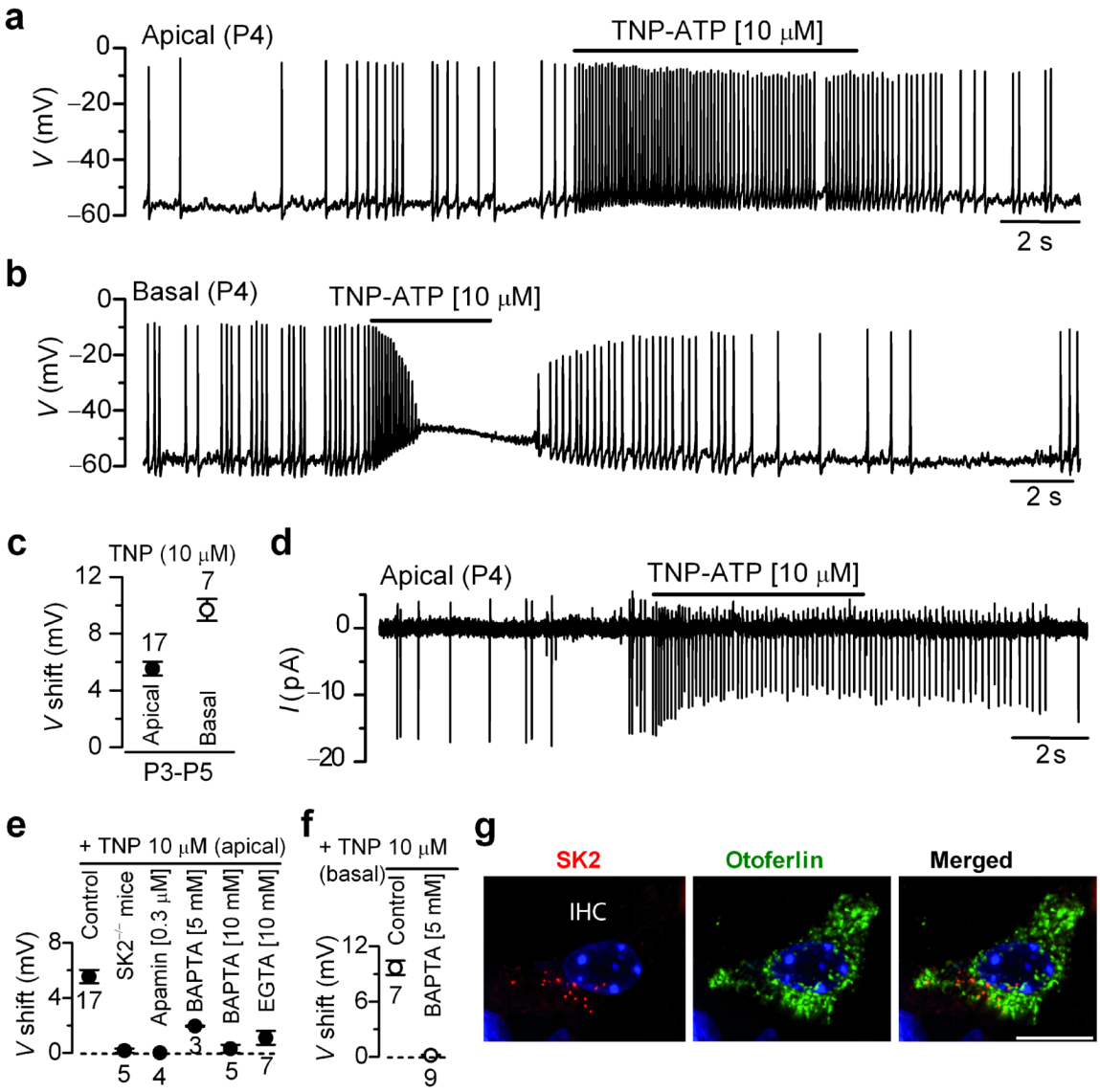

Figure 5. Role of endogenous ATP in spontaneous spiking activity in mouse IHCs

(**a** and **b**), Spontaneous APs recorded with whole-cell current clamp from apical and basal IHCs, respectively, during superfusion of TNP-ATP. Note the increased frequency and decreased height of APs during the application of TNP-ATP, with basal IHCs being more affected than apical cells. (**c**), Depolarizing shift in V_m of apical and basal IHCs during the superfusion of TNP-ATP. (**d**), Spontaneous cell-attached spikes recorded from a mouse IHC in the presence of TNP-ATP. (**e**), Comparison of V_m shift when apical P3-P5 IHCs were superfused with TNP-ATP alone or together with the SK2 channel blocker apamin (both with 1 mM intracellular EGTA), in SK2 knockout mice ($SK2^{-/-}$) or when the intracellular Ca^{2+} buffers BAPTA (5-10 mM) or EGTA (10 mM) were used. The experiments with 10 mM EGTA were performed at room temperature. (**f**), V_m shift when basal IHCs were perfused with TNP-ATP alone or in the presence of 5 mM intracellular BAPTA. (**g**), Apical immature IHC immunostained for SK2 channels (red) and the IHC marker otoferlin (green). Nuclei were stained with DAPI (blue). Scale bar: 10 μM

Europe PMC Funders Author Manuscripts

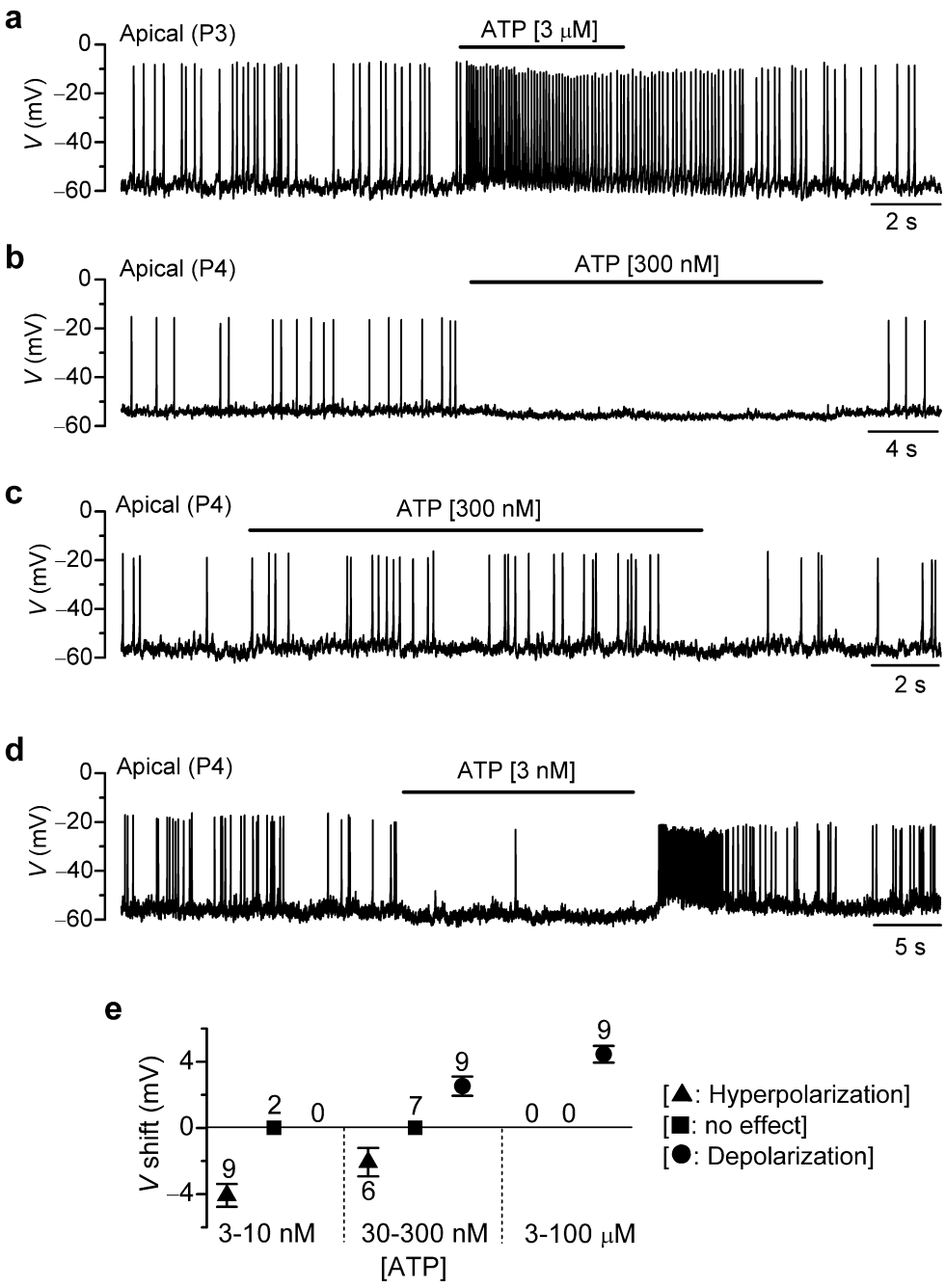

Figure 6. Dual action of ATP on spontaneous spiking activity in mouse IHCs

(**a**), Spontaneous action potentials recorded with whole-cell current clamp from an apical IHC. Extracellular application of 3 μM ATP caused IHC depolarization. (**b** and **c**), High nanomolar concentrations of ATP had mixed effects on IHC V_m, with some cells showing a small hyperpolarization (**b**) and others exhibiting a small depolarization (**c**: slightly increased action potential frequency). (**d**), Low nanomolar concentrations of ATP (3 nM) caused IHC hyperpolarization. Note that in some cases following ATP application a small depolarizing rebound occurred before the IHC returned to a stable V_m. (**e**), V_m shift in response to different ATP concentrations.

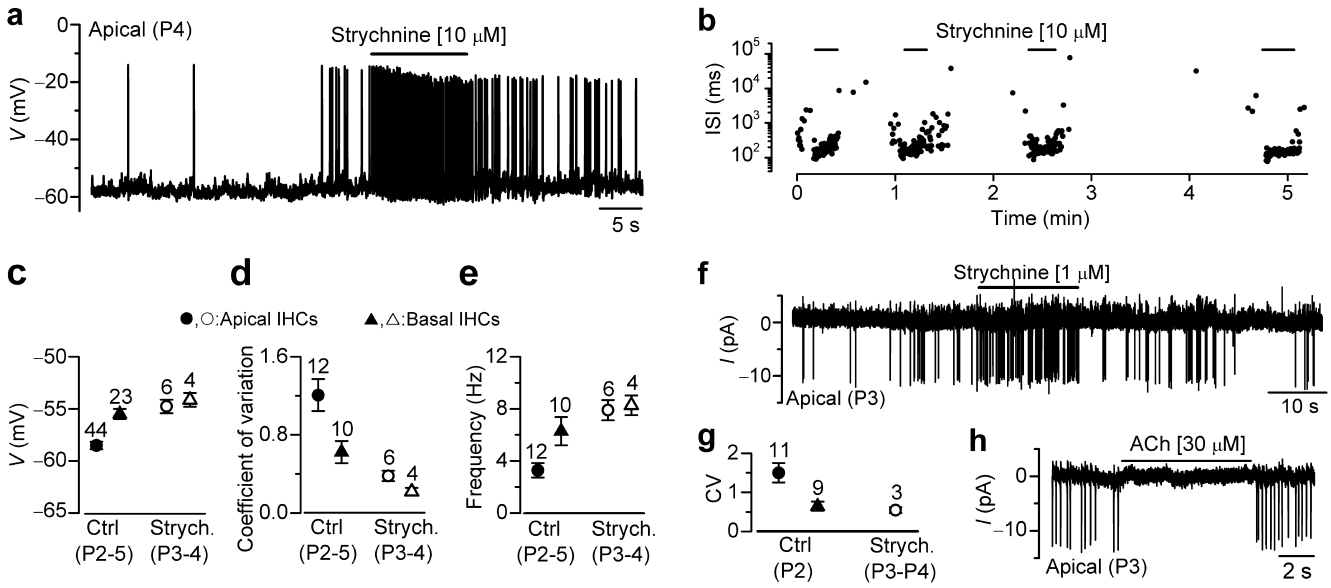

Figure 7. Effect of endogenous ACh on IHC spontaneous spiking activity

(**a**), Spontaneous whole-cell action potentials from an apical P4 IHC with the superfusion of 10 μM strychnine, a specific α9α10 nAChR blocker. Strychnine caused a small IHC depolarization, which increased the action potential frequency. (**b**), ISIs as a function of time from the same apical IHC shown in **a**. Note the periodic increases in spiking rate with strychnine in between silent/reduced activity. (**c-e**), V_m (**c**), coefficient of variation (**d**) and frequency (**e**) of action potentials in control conditions and with 1 μM or 10 μM strychnine measured from P2-P5 apical and basal IHCs. For all three panels, significant differences were only observed between apical control IHCs and the other conditions (overall significance from one-way ANOVA: V_m $P < 0.0001$; coefficient of variation and frequency $P < 0.005$). (**f**), Cell-attached spikes showing increased firing activity in the presence of 1 μM strychnine. (**g**), As shown for whole-cell recordings (**d**), in the presence of strychnine the coefficient of variation (CV) of cell-attached spike ISIs in apical IHCs was significantly lower than control apical cells ($P < 0.05$) but similar to that of control basal cells. (**h**), Cell-attached spikes are abolished during the application of the inhibitory efferent neurotransmitter ACh.